Multidirectional Illuminating Optical Fiber Tip on Beam Expanding Coreless Silica Fiber

Jun Ki Kim, Jin Woo Choi, Anka Schwuchow, Hartmut Bartelt, Tae-Hun Kim, Woo June Choi, Jae Young Kim, Dong Uk Kim, Seon Young Ryu, Geon Hee Kim, Ick-Hee Kim, and Ki Soo Chang

***Abstract*— We report a compact all-optical side-firing probe directly ablated on a mode-expanded hybrid fiber end using a high-precision femtosecond laser processing technique. A segment of coreless silica fiber was adopted to achieve a large beam size and manipulation of the far field divergence angle. The radiating beam properties of the side-firing tip have been experimentally investigated and compared with numerical simulations.**

***Index Terms*— Side-firing probe, side emitting fiber, laser ablation, coreless silica fiber (CSF).**

I. Introduction

UNLIKE a frontal emitting configuration, in which light is emitted only along the optical axis, a side-emitting probe is a very useful scheme for biomedical applications such as *in vivo* imaging, laser surgery, laser scanning, lithotripsy, and photodynamic therapy (PDT). Compactness and high system efficiencies can be achieved using the side-emitting scheme. For example, in microsurgery in a tubular structure such as the urethra or microvasculature requires an accurate removal of lesions using precise laser beam control. However, it is difficult for the laser beam to reach the side wall of the tubular structure in the frontal emitting scheme [1]. Even under illumination of a large area as used in lithotripsy or PDT, randomly scattered light from the tip of a single-mode fiber based on frontal direction illumination is not sufficient to reach every nook and corner of the target area [2], [3].

For side-directional illumination, metal reflectors have been used for medical operations such as prostatectomies [4]. Although it demonstrates good reflectivity, heat generation on the metal surface makes this method inadequate for applications in the human body. To solve the light guidance and overheating problems simultaneously, optical fibers have been adopted as a new transitional tool. Side-illuminating fibers have been introduced as types of surface-emitting fiber lasers [5] and side glowing fibers [6], [7]. Although these are good illuminating devices, their methods require a sophisticated fabrication process both before and after the fiber drawing, which results in high manufacturing cost. In addition, it is hard to control the illuminating area, and there are even emissions in unnecessary zones because these devices do not have a probe tip.

Recent high-precision laser processing techniques using a femtosecond laser for direct inscription of optical fibers have a competitive edge in terms of both price and technological superiority. The extremely high peak power of a femtosecond laser allows precise ablation of various materials, such as metals, semiconductors, and dielectric materials [8]–[10]. Choi *et al*. reported side-viewing probes on a ball lens tip after femtosecond laser machining [11]. However, the illuminating area was confined to a limited section. To create a multidirectional-firing optical probe tip, microstructuring of a large-core optical fiber using a femtosecond laser has been recently proposed by the authors [12]. However, the proposed construction is still restricted in its control of the directions of the emitted beam due to a fixed core diameter, which limits the degrees of freedom of the device. Further, for practical applications, a detailed theoretical analysis should be included, since precise diverging beam handling is indispensible for data quantification with concrete parameters.

In this letter, a novel technique is demonstrated by combining a hybrid fiber mode-expansion method and a high-precision femtosecond laser ablation process, making manipulation of the emitted beam possible. It is simple, easy to make and cost effective. We can adjust beam divergence angle by changing several parameters. The characteristics of the side-emitting fibers can be experimentally investigated and compared with the results of numerical simulations.

II. Experiments and Results

The hybrid structure is composed of a coreless silica fiber (CSF) serially fusion-spliced with a high-power small-core (HPSC) multimode fiber (MMF). The HPSC fiber (NA = 0.10) is designed for high-power applications, including high-power laser transmission. The core and cladding diameters are 10 μm and 125 μm, and the refractive indexes of the core and cladding are 1.457 and 1.453 at 633 nm, respectively. A schematic diagram of the proposed device is given in Fig. 1. Light exiting the MMF propagates along the CSF, which has a refractive index of 1.44 and

Manuscript received September 2, 2013; revised October 4, 2013; accepted October 23, 2013. Date of publication November 4, 2013; date of current version November 19, 2013. This work was supported in part by the Korea Basic Science Institute under Grant D33200, in part by SMBA under Grant S2060032, and in part by the INNOPOLIS supporting program of MKE under Grant 1414119537.

J. K. Kim, W. J. Choi, J. Y. Kim, D. U. Kim, S. Y. Ryu, G. H. Kim, and K. S. Chang are with the Korea Basic Science Institute, Daejeon 305-806, Korea (e-mail: ksc@kbsi.re.kr).

J. W. Choi is with the Wonkwang University, Iksan 570-749, Korea.

A. Schuwuchow and H. Bartelt are with IPHT, Jena 07745, Germany.

T.-H. Kim is with the Agency for Defense Development, Daejeon 305-152, Korea.

I.-H. Kim is with Kunkuk University, Chungju 380-701, Korea (e-mail: uuu220@kku.ac.kr).

Color versions of one or more of the figures in this letter are available online at http://ieeexplore.ieee.org.

Digital Object Identifier 10.1109/LPT.2013.2287877

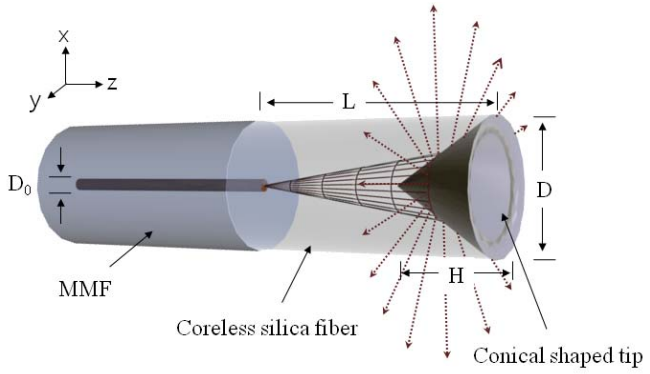

Fig. 1. Schematic diagram of light propagation after engraving a conical shape on the surface of coreless silica fiber (CSF), where L is length of CSF; H is height of cone; D, D_0 are the diameter of cladding and core, respectively.

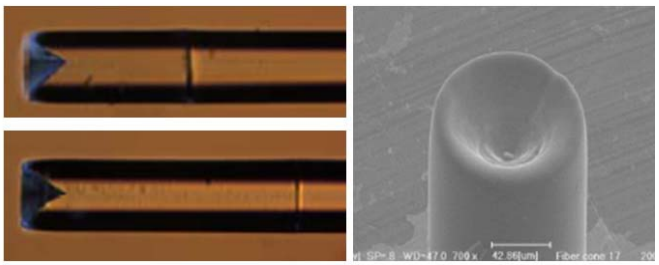

Fig. 2. Microscope images of the fabricated probe (left) (Top: Length of CSF L = 300 μm; Bottom: L = 500 μm); SEM image of the polished tip after arc discharging (right).

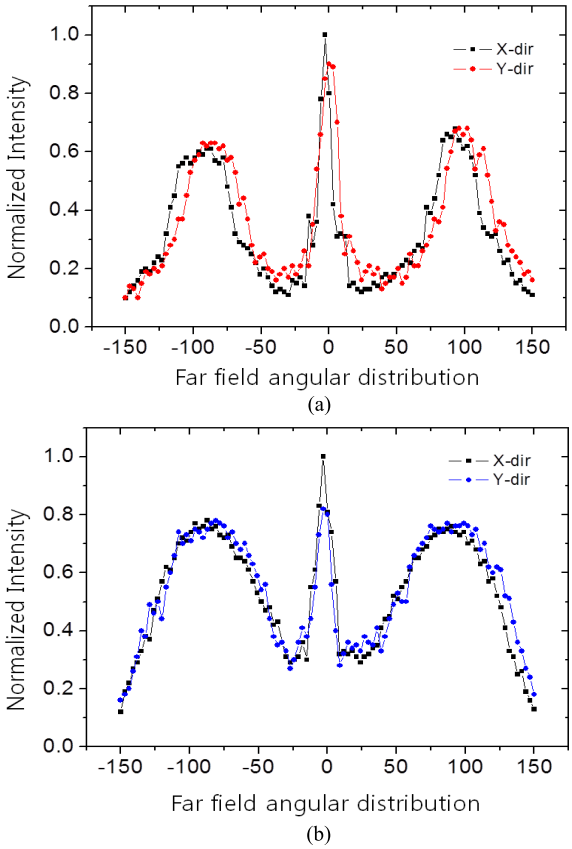

Fig. 3. Normalized far field intensity distribution with far field angle; (a) L = 300 μm; (b) L = 500 μm.

serves as a homogenous propagation medium [13], [14] with a divergence angle corresponding to the numerical aperture. Using femtosecond laser ablation, a conical shaped tip is engraved on the surface of CSF. An amplified Ti:Sapphire laser operating with a wavelength of 785 nm and a 185-fs pulse duration was utilized at a repetition rate of 1 kHz with a maximum output power of 1 W. After aligning the objective lens (NA = 0.4) over the CSF surface, the engraving of the conical shape was made by producing multiple disk patterns at different depths of the tip. To remove scattering and the diffusion of the reflection at the surface of engraved multiple disk patterns, an arc discharging process was performed on the conical shaped tip using a fiber splicer (Vytran, CAS-4100). The applied power and arc duration were 75 W and 2800 ms, respectively. Detailed machining and arc discharging procedures are described elsewhere [12].

Fig. 2 shows optical microscopy and scanning electron microscopy (SEM) images of the fabricated side-firing probe after the arc discharge process. The depth corresponding to the height of the cone (H) was chosen to be 80 μm to satisfy the total internal reflectivity (TIR) condition with the given NA. The angle of the cone was 71.4°.

For CSF lengths that are greater than a certain length, interferences will occur between the light from the core of the MMF and the reflected light from the cylindrical surface of the CSF, and such interferences will interrupt the TIR condition, resulting in the occurrence of unintended frontal beam emission. Thus, L_{Max}, the maximum length of the CSF that will not generate interferences, is determined by

$$L_{Max} = \left(\frac{D - D_0}{2\tan\theta}\right) \tag{1}$$

where, $\theta = \arcsin(NA)$ and where D and D_0 are the diameters of the cladding and core, respectively.

Based on Eq. (1), we calculated that the maximum CSF length was 572 μm at the given values for the NA and the diameters of the core and cladding.

By varying the geometrical dimensions of CSF, the proposed composite fiber-optic device can provide very versatile and flexible control in terms of beam divergences. Thus, we fabricated two different types of probe with different CSF lengths (Fig. 2) to confirm the flexible control. The divergence properties of the beam were investigated by launching a He-Ne laser beam into the proposed hybrid structure. Fig. 3 shows the normalized intensity distribution of the far field around the fabricated probes measured by rotating a far field intensity measurement system (Hamamatsu A3267-11). Owing to its cylindrical structure, we selected two representative directions, the X- and Y-axes, and compared the divergence properties between them. The X- and Y-axes are two perpendicular axes, and the XY plane is also orthogonal to the Z-axis. The optical intensities were scanned in the X- and Y-directions using goniometry. We clearly confirmed that the case of the longer CSF had a wider distribution angle around the probe, since there was a larger area of contact at the cone

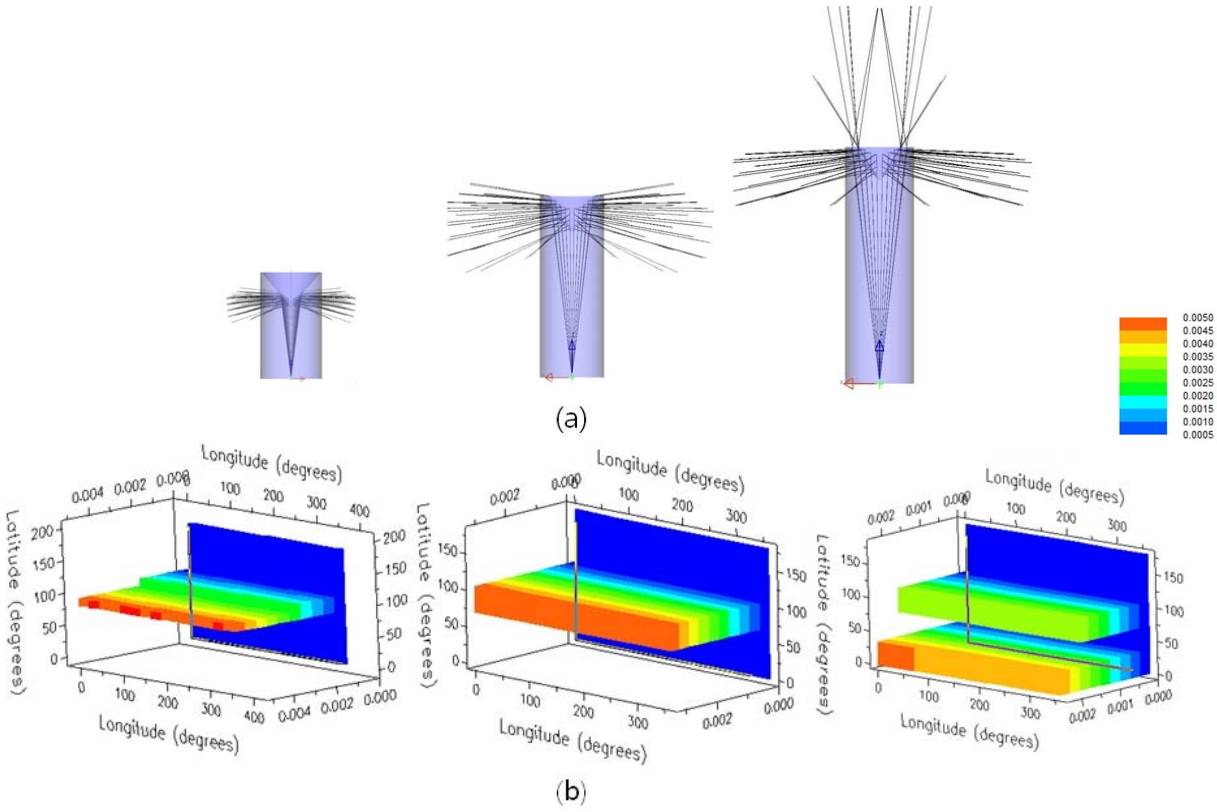

Fig. 4. Simulation results for the designed side-firing optical probe utilizing a commercial optical simulation tool, Light ToolsTM. (a) Side view of the beam propagation along the length of the CSF, L = 300 μm (left); L = 500 μm (middle); L = 700 μm (right). (b) Radiant intensity chart along the length of the CSF, L = 300 μm (left); L = 500 μm (middle); L = 700 μm (right).

at the intersection between the source beam and the engraved surface.

Compared to the CSF length of 300 μm, a wider diverging angle was measured with a CSF length of 500 μm. The averaged full width at half maximum intensity (FWHM) of the left/right lobe in Fig. 3 was distributed in the range of 42° in Fig. 3-(a) and 92° in Fig. 3-(b). It seems that the scattered remains on the engraved CSF surface due to the imperfection of the arc discharge process generate central intensity lobes. The deviations between the X-axis and Y-axis in each case are mainly attributed to the asymmetric cone structure formed during laser ablation. However, these results are reasonable enough to confirm that a side-firing optical probe inscribed on CSF could show good side directional illumination and provide flexibility with a high degree of freedom of the system.

The beam propagations after reflection at the engraved surface were also theoretically investigated utilizing a commercial optical simulation package, LightTools^{TM}. In the simulation tool, actual dimensions were used, and the reflected beam from the given structure was investigated in terms of the radiance intensity distribution using illumination analysis. The illumination analysis in LightTools is based on a Monte Carlo ray trace [15], which traces the desired number of rays from randomly selected points on the surface or volume into randomly selected angles in space. The side view of the beam propagation and the radiant intensity chart results for several types of engraved structures are shown in Fig. 4(a) and (b), respectively. As the longitudinal position (longitude axis) varies over 2π (0° to 360°) around the probe tip, each case has a unique latitudinal divergence angle (latitude axis) and intensity distribution (color map) in Fig. 4-(b). The simulation results showed good agreement with the experimental measurements in terms of the divergence angle of the beam, with a 38° divergence angle for the CSF length of 300 μm and an 80° divergence angle for the CSF length of 500 μm.

Beyond a certain CSF length, interference between the central light emitted from the MMF and reflected light from the cylindrical surface of CSF will be generated. This will interrupt the TIR condition, resulting in frontal beam emission. By applying a longer CSF structure (Fig. 4-(c) L = 700 μm), over the maximum length of CSF that will not generate interference patterns, we also found that frontal emitting divergences can be controllable, which makes the device potentially suitable for many future applications.

III. Conclusion

In summary, we have demonstrated the fabrication of an all-fiber side-firing optical probe inscribed on an optical fiber end face using a femtosecond laser. A CSF (coreless silica fiber) segment has been spliced after the MMF to provide an expanded modal field whose intensity distribution can be further tailored by altering the CSF length and reflected area. The far field divergence properties of the side-firing probe were investigated by directing a He-Ne laser beam into the

optical fiber. Utilizing a Monte Carlo ray tracing package, beam propagations from devices were simulated and showed good agreement with experimental results. By attaching robust sheath over the probe, we could apply proposed device into practical applications such as laser surgery, lithotripsy or PDT. Thus, the proposed device has ample potential for use in various bio-photonics and bio-medical fields because of its high degree of freedom.

REFERENCES

[1] J. K. Kim, *et al.*, "Fabrication and operation of GRIN probes for in vivo fluorescence cellular imaging of internal organs in small animals," *Nature Protocol.*, vol. 7, no. 8, pp. 1456–1469, Aug. 2012.

[2] R. L. Blackmon, P. B. Irby, and N. M. Fried, "Thulium fiber laser lithotripsy using tapered fibers," *Lasers Surgery Med.*, vol. 42, no. 1, pp. 45–50, Jan. 2010.

[3] K. Miyazaki, *et al.*, "A novel homogeneous irradiation fiber probe for whole bladder wall photodynamic therapy," *Lasers Surgery Med.*, vol. 44, no. 5, pp. 413–420, Jul. 2012.

[4] C. F. van Swol, R. M. Verdaasdonk, R. J. van Vliet, D. G. Molenaar, and T. A. Boon, "Side-firing devices for laser prostatectomy—A review," *World J. Urol.*, vol. 13, no. 2, pp. 88–93, Apr. 1995.

[5] O. Shapira, *et al.*, "Surface-emitting fiber lasers," *Opt. Express*, vol. 14, no. 9, pp. 3929–3935, May 2006.

[6] (2013, Jun. 11). *Side-Glowing Fiber* [Online]. Available: http://www.somta.lv/wp30.htm

[7] (2013, Jun. 11). *Side-Emitting Fiber* [Online]. Available: http://www.meshtel.com

[8] M. Halbwax, *et al.*, "Micromachining of semiconductor by femtosecond laser for integrated circuit defect analysis," *Appl. Surf. Sci.*, vol. 254, no. 4, pp. 911–915, Dec. 2007.

[9] R. Martinez-Vazquez, R. Osellame, G. Cerullo, R. Ramponi, and O. Svelto, "Fabrication of photonic devices in nanostructured glasses by femtosecond laser pulses," *Opt. Express*, vol. 15, no. 20, pp. 12628–12635, Oct. 2007.

[10] I. B. Sohn, M. S. Lee, J. S. Woo, S. M. Lee, and J. Y. Chung, "Fabrication of photonic devices directly written within glass using a femtosecond laser," *Opt. Express*, vol. 13, no. 11, pp. 4224–4229, May 2005.

[11] H. Y. Choi, *et al.*, "Single-body lensed photonic crystal fibers as side-viewing probes for optical imaging systems," *Opt. Lett.*, vol. 33, no. 1, pp. 34–36, Jan. 2008.

[12] I. B. Sohn, Y. S. Kim, Y. C. Noh, I. W. Lee, J. K. Kim, and H. Lee, "Femtosecond laser and arc discharge induced microstructuring on optical fiber tip for the multidirectional firing," *Opt. Express*, vol. 18, no. 19, pp. 19755–19760, Sep. 2010.

[13] J. K. Kim, M. Han, S. Chang, W. J. Lee, and K. Oh, "Achievement of large spot size and long collimation length using UV curable self-assembled polymer lens on a beam expanding core-less silica fiber," *IEEE Photon. Technol. Lett.*, vol. 16, no. 11, pp. 2499–2501, Nov. 2004.

[14] J. K. Kim, *et al.*, "Fabrication of micro Fresnel zone plate lens on a mode-expanded hybrid optical fiber using a femtosecond laser ablation system," *IEEE Photon. Technol. Lett.*, vol. 21, no. 1, pp. 21–23, Jan. 1, 2009.

[15] *Illumination Module User's Guide*, Opt. Res. Assoc., Pasadena, CA, USA, 2003.